**Large scale pantelleritic ash flow eruptions during the Late Miocene in central Kenya and evidence for significant environmental impact**

Claessens, L.[a,d], Veldkamp, A.[b], Schoorl, J.M.[a], Wijbrans, J.R.[c], van Gorp., W[a], Macdonald, R.[e,f]

[a] Soil Geography and Landscape group, Wageningen University, P.O. Box 47, 6700 AA Wageningen, the Netherlands

[b] Faculty ITC, University of Twente, P.O. Box 217, 7500 AE Enschede, the Netherlands

[c] Department of Earth Science, Vrije Universiteit, De Boelelaan 1085, 1081 HV Amsterdam, the Netherlands

[d] International Crops Research Institute for the Semi-Arid Tropics (ICRISAT), P.O. Box 39063, 00623 Nairobi, Kenya

[e] Environmental Science Division, Lancaster University, Lancaster LA1 4YQ, UK

[f] IGMiP Faculty of Geology, University of Warsaw, 02-089 Warszawa, Poland

[*] Corresponding author: Lieven Claessens, International Crops Research Institute for the Semi-Arid Tropics (ICRISAT), P.O. Box 39063, 00623 Nairobi, Kenya. Phone: + 254 20 722 4568. Email: l.claessens@cgiar.org

## Abstract

In the area south-east of Mount Kenya, four previously unrecorded peralkaline rhyolitic (pantelleritic) ash flow tuffs have been located. These predominantly greyish welded and non-welded tuffs form up to 12 m thick units, which are sometimes characterized by a basal vitrophyre. The four flow units yielded $^{40}Ar/^{39}Ar$ ages ranging from 6.36 to 8.13 Ma, indicating a period of ~1.8 Ma of pantelleritic volcanic activity during the Late Miocene in central Kenya. Tentative compositional and age correlations with other known tuff deposits suggest that the pantelleritic tuffs originally covered 40,000 km$^2$ in central Kenya, extending much further than earlier recorded Pliocene tuffs. This newly identified magmatic phase occurred between the phonolitic flood eruptions (16-8 Ma) and the Pliocene tuff eruptions (6-4 Ma). The occurrence of multiple ash flow tuff deposits up to 150 km away from the inferred eruptive center(s) in the central sector of the

Kenya Rift, indicates multi-cyclic peralkaline supereruptions during the Late Miocene. By analogy with more recent pantelleritic eruptions, the tuffs are thought to have been sulphur-rich; during eruption, they formed stratospheric aerosols, with significant environmental impact. The timing of the eruptions coincides with the shift towards more savannah-dominated environments in East Africa.

**Keywords**: tuff, ash flow, ignimbrite, vitrophyre, peralkaline rhyolites, $^{40}Ar/^{39}Ar$ geochronology

## 1. Introduction

The onset of uplift, rifting and associated volcanism in East Africa was recently constrained by the (re)discovery of a 17 Ma old whale fossil in the Turkana region in northern Kenya 740 km inland from the present-day coastline of the Indian Ocean at an elevation of 620 m (Wichura et al., 2015). Since its formation during the Miocene, the Kenya Rift Valley has been estimated to have erupted more than 150,000 km$^3$ of volcanic rocks (Smith, 1994). The majority of these eruptives belong to the Plateau phonolites phase that erupted between 16 and 8 Ma ago (Macdonald, 2003). In the central sector of the Kenya Rift this phase was followed by a more explosive phase depositing thick (100-300 m) sequences of welded and non-welded ash flows and air-fall tuffs, labeled 'Pliocene tuffs'(Smith, 1994; Fig. 1-A). A first broad correlation suggests that an area of 29,000 km$^2$ was covered by these deposits and that the ash flows were sourced in the Nakuru-Naivasha-Suswa area (McCall, 1967; Baker et al, 1988; Leat, 1991; Smith, 1994). The so-called 'Pliocene tuffs' cover a roughly circular area centered by Lake Naivasha and with a radius of approximately 90 km (Fig. 1). Various different tuff deposits are recognized with only a handful of reliable age determinations that range from 6.4 to 4.2 Ma (Jones and Lippard, 1979). The oldest dated tuffs are the Mau tuffs which consist of at least four ash flow units of peralkaline trachytic composition. The youngest two flows have K-Ar ages of 6.0-5.8 Ma (Jones and Lippard, 1979) indicating late Miocene emplacement. Despite these clear late Miocene ages, Smith (1994) assembled all mainly trachytic (alkalis-silica classification; Le Bas et al., 1992) tuff deposits and defined them as 'Pliocene tuffs', heavily relying on the correlation of all eastern tuffs, specifically the Kinangop tuff (5.7-3.4 Ma) in the Kinangop plateau (Baker et al., 1988). Other accurate $^{40}Ar/^{39}Ar$ age estimates of tuffs and related deposits were obtained at hominid sites such as the Tugen Hills (Kingston et al., 2002) and near Lake Turkana, where Late Miocene and Pliocene tuffs have been dated (Brown and McDougall, 2011). All these tuffs are considered to have originated in the central sector of the Kenyan Rift from several potential eruptive centers (Smith, 1994). During geological mapping of the area south and south-east of Mount Kenya, different tuff deposits were described (Bear, 1952; Fairburn, 1963, 1966). The tuffs are partly buried by predominantly phonolitic lava flows and volcanic debris avalanche deposits (agglomerates) of Mount Kenya, indicating an older origin. The main volcanic activity of Mount Kenya has recently been dated accurately and occurred between 5.27 and 2.8 Ma ($^{40}$Ar/ $^{39}$Ar; Veldkamp et al., 2012; Schoorl et al., 2014). Somehow, these extensive tuff deposits have been ignored in Mio-Pliocene volcanic reconstructions. Given their location approximately 150 km east of the Kenya rift-axis, these tuffs can only have been deposited from large-scale, disruptive eruptions and may provide important information on distinct environmental changes and may be useful for paleogeomorphological reconstructions of the region.

In order to resolve the origin and age of the tuffs south-east of Embu, exposures were mapped and sampled for geochemical analysis and $^{40}$Ar/ $^{39}$Ar dating. This paper aims to characterize the tuffs and to relate them to the Late Cenozoic geological and paleoenvironmental history of central Kenya.

**Study area**

The study area is located in central Kenya and encompasses the eastern part of Embu County. Geological features in that setting include Mount Kenya volcanic deposits in the north and exposed Proterozoic metamorphic and crystalline rocks of the Mozambique Belt in the east and south (Bear, 1952; Fairburn, 1963; Veldkamp and Visser, 1992; Fig. 1-A). In the area south-east of Embu, volcanic tuffs have been found adjacent to, and below, Mount Kenya volcanic rocks (Bear, 1952; Fairburn, 1966; Fig. 1-A). These volcanic deposits have been correlated to the undated Nyeri tuffs and their origin has been preliminarily suggested in the Aberdares (Fairburn, 1966). More to the south, in the area north of Machakos and east of Thika, Fairburn (1963) mapped similar tuffs, which he referred to as the Athi tuffs. Later Baker et al., (1971, p. 199-200) correlated all these tuffs to the Plio-Pleistocene trachytic group.

Direct age estimates of the tuffs do not exist and only very tentative correlations have been explored. A palaeogeomorphological reconstruction of the Pliocene upper Tana basin raised questions about the age of the observed tuffs. It was suggested that some of the tuffs could have been related to main blocking phases of the Tana River (Veldkamp et al., 2012). This would imply

Pliocene ages (around 4 Ma) for the deposits. Based on this landscape reconstruction it is now also known that the volcanic debris avalanche (VDA) deposits of Mount Kenya overlying the tuffs south of Embu are around 2.8 Ma old (Schoorl et al., 2014).

Interestingly, the tuffs are found only above an elevation of 1100 m. All lower topographic features are integral parts of the erosional Tana valley, which started to incise at 2.8 Ma (Veldkamp et al., 2007). The Tana River has incised a 160 m deep valley, in which gravelly fluvial strath terraces with Quaternary ages have been recognized (Veldkamp et al., 2007). Due to the fluvial reorganizations of the upper Tana basin caused by a major volcanic debris avalanche event (around 2.8 Ma; Schoorl et al., 2014) and the emplacement of the Thiba flood basalt (0.8 Ma; Veldkamp et al., 2012), the Tana valley shifted southwards - and maintained the preservation of the tuff-containing area from further erosion.

## 2. Samples and Methods

### *2.1 Fieldwork*

Fieldwork consisted of an inventory, starting with previously mapped tuffs (Bear, 1952) and leading to the discovery of new deposits during different field campaigns (2008-2010, 2012, and 2014; Fig. 1-B). Table 1 gives a summary of the key locations discussed in this study. All encountered tuff units were sampled for $^{40}Ar/^{39}Ar$ dating and geochemical analysis. Samples were taken from fresh, non-weathered massive rock outcrops in building stone quarries. Local geomorphological mapping was based on a 30 m hole-filled seamless Shuttle Radar Topography Mission Digital Elevation Model (SRTM DEM; Reuter et al., 2007; Jarvis et al., 2008). In the field, hand-held GPS devices were used to register coordinates and altitudes of the sampling locations. The Universal Transverse Mercator (UTM) coordinates were linked to the SRTM DEM. In this study the DEM altitudes were used to establish altitudes of locations.

#Fig. 1 approx. here

#Table 1 approx. here

### *2.2 $^{40}Ar/^{39}Ar$ dating*

Samples were collected for $^{40}Ar/^{39}Ar$ dating from all four tuffs (see Fig. 1 and 2 for sample locations). Age estimates were obtained by incremental heating experiments carried out at the VU University, Amsterdam, the Netherlands (Schneider et al., 2009). Groundmass separates were prepared by obtaining homogenous fragments of microcrystalline groundmass to minimize the possibility of inherited argon from phenocryst phases (Wijbrans et al., 2011). For one sample (Ngandurea upper tuff) the sanidine phenocrysts were separated and dated separately. Data reduction and age calculations were made using ArArCalc v2.5 (Koppers, 2002). The detailed procedure is described in van Gorp et al. (2013), and Schoorl et al. (2014). Geochemical analyses were carried out at Activation Laboratories in Lancaster, Canada, using Fusion Inductively Coupled Plasma Emission (FUS-ICP). Subsequently, the methods can be found at http://www.actlabs.com/ .

## 3. **Results**

### *3.1 Site descriptions*

Four key sites were identified and studied in detail (Fig. 1; Table 1). Schematic cross-sections of the four sites are visualized in Figure 2. In the original map by Bear (1952), seven patches of tuff deposits were large enough to be mapped. One of the map units was mistakenly attributed to the here investigated tuffs. However, this unit is in fact a bottomland in the 2.8 Ma volcanic debris avalanche deposit (Schoorl et al., 2014). Originally Bear (1952) distinguished between two distinct tuff types: (a) a melanocratic gritty tuff north of Siakago (site A; Fig. 1-B and 2-A) and (b) a pale-grey homogeneous tuff at Ngandurea (site B; Fig. 1-B and 2-A). We revisited both key sites, and extended our study objects by two more tuff localities: (c) Gikiiro (site C; Fig. 1-B and 2-B) and (d) Mavurea (site D; Fig. 1-B and 2-B). The latter are building stone quarries, which provide sufficient outcrops and exposures to describe and sample the tuffs.

#### *3.1.1 Site A: Siakago*

An 11 m thick tuff crops out along the road (active and former building stone quarries) and in the river between an altitude of 1138 and 1149 m (Fig. 1-B). The tuffs comprise two units, the upper and lower tuffs, separated by a basal vitrophyre in the upper tuff. Both tuffs are grey massive, homogeneous and show weak columnar jointing (Fig. 2). The upper tuff (Fig. 3) is pale grey and demonstrates a clear orientation of flattened pumice fragments. The base of this unit consists of a vitrophyre up to one meter thick (Fig. 3). Towards the north and east, the tuffs are buried by the 2.8 Ma Mount Kenya volcanic debris avalanche deposits (Schoorl et al., 2014). The lower tuff

(Fig. 4) is dark grey and contains volcanic and non-volcanic lithic fragments, which are often rounded and follow the descriptions by Bear (1952) of the melanocratic gritty tuff. The base of the lower tuff is not clearly exposed, but no indications of glass were found near its base. A well-sorted greenish fluvial sand was observed at one location.

### *3.1.2 Site B: Ngandurea*

Near the village of Ngandurea the tuffs form a long elongated, flat tilting terrace bench (6 x 2 km) between an altitude of 1221 and 1149 m. This prominent feature west of the granitic Kanjiro hill exhibits the largest visible tuff unit (Fig. 1). Along the edge many building stone quarries occur. Almost all the quarries mine the massive pale-grey homogeneous upper tuff (Fig. 2 and 5). The Ngandurea upper tuff forms a continuous, 5 to 7 m thick, unit that strongly resembles the Siakago upper tuff. The tuff has only a few lithic clasts embedded in a pale greyish groundmass carrying numerous microlites and displays clearly oriented flattened pumice fragments (Fig. 5). Twig and wood imprints are occasionally found (Fig. 6). Welding in these tuffs is commonly associated with streaks of obsidian or pumice fragments flattened parallel to the bedding. Towards the base of the tuff, more glass is observed and at some locations a 0.3 to 1 m thick massive vitrophyre forms the base of the Ngandurea upper tuff (Fig. 5). Fluvial gravels were found at a location where the Ngandurea tuff directly overlies basement system gneisses, indicating preservation in a former valley. Towards the south, the Ngandurea upper tuff (6 m) directly overlies granitic slope material and a reddish palaeosol formed in an underlying tuff (> 6m), which is grey lower down which strongly resembles the Siakago lower tuff (Fig. 4 and 7). This tuff has a reddish/pinkish greyish colour at the top which becomes grey in the deeper parts of the unit (Fig. 7). The tuff does not display the same pumice orientation as the Ngandurea upper tuff (Fig. 5). It is rich in volcanic lithic fragments (dark basaltic to whitish pumice clasts), which are often rounded and less massive than in the overlying upper tuff. The base of this older tuff was not clearly exposed although no glass was observed near the base. Some gravels were found on the slope near the tuff-basement contact, again indicating deposition in a former valley. The total maximum accumulated thickness of the two tuff units is 13 m.

### *3.1.3 Site C: Gikiiro*

Near Gikiiro the tuff crops out in various building stone quarries on the slope of a phonolite-capped hill at an altitude of 1218 m (Fig. 1.B and Fig. 2). These tuff outcrops occur all around the hill slope, indicating that the overlying 22 m thick dark Kari phonolite (3.9 Ma; Veldkamp et al., 2012) infills a shallow valley incised into the tuffs. Locally gravels are observed near the base of the phonolitic lava flow. Figure 8 shows the Kari phonolite overlying a 0.4 m thick sandy palaeosol (with hydromorphic features) in slope material developed on top of the Gikiiro tuff. The Gikiiro tuff itself is a massive greyish tuff with no clear clast orientation and poor in lithic fragments. At the base a coarse, rounded pumice-rich unit occurs (Fig. 8). The maximum exposed thickness of the Gikiiro tuff is 5 m.

#### *3.1.4 Site D: Mavurea*

The Mavurea tuff (Fig. 1.B and Fig. 2) is exposed at only one locality where numerous small building stone quarries of maximum 5 m depth are found between an altitude of 1150 and 1158 m. The total thickness is about 8 m but no single outcrop exposes the entire unit. The base comprises a thick continuous and massive vitrophyre layer of approximately 1 m thickness (Fig. 9). The Mavurea tuffs have only a few irregular inclusions of foreign material (mainly wood and reed imprints and some un-orientated pumice fragments) embedded in a light greyish groundmass. The top of the unit is strongly cemented by ironstone and is overlain by sandy deposits containing murram (Fig. 9).

### *3.2 Geochemistry*

Chemical analyses of the tuffs are presented in Table 2.

#Table 2 approx. here

When the tuffs are classified using the alkalis-silica classification scheme, the Siakago lower tuff is considered as a dacite/trachyte, the Ngandurea upper tuff and the Gikiirro tuff as a trachyte, and the Mavurea tuff as a rhyolite. However, a problem in the analysis of pyroclastic rocks is that they are very prone to secondary hydration and consequent compositional modifications, especially the loss of Na and gain of Ca. The high loss of ignition values (up to 4.75 wt.%), indicate that the studied tuffs have been hydrated, with significant loss of Na. Non-hydrated rocks of similar composition contain >6 wt.% of $Na_2O$, as compared to the recorded values of <5 wt.%.The loss of Na is important because it affects such features as the CIPW normative composition, the composition of the normative feldspar, and the rock classification on the total alkalis – silica plot (Le Bas et al., 1992).

The CIPW normative compositions (Table 2) demonstrate that none of the samples have normative corundum but they do have acmite with sodium metasilicate (ns), which is a measure of peralkalinity. Using the approach after Macdonald et al. (1987) for peralkaline silicic rocks, the tuffs have 24-30% normative quartz and are acmite-normative, indicating that they are peralkaline rhyolites. Following Macdonald's (1974) $FeO_{tot}$–$Al_2O_3$ diagram of peralkaline rhyolites, the tuffs are pantellerites, compositionally similar to the pantellerites from the type-locality, the island of Pantelleria, Italy (Fig. 10-A). In this diagram, the Siakago lower tuff is slightly more aluminous than the others, indicating derivation from a different magma. Differences between the tuffs are also seen in the trace element data; whilst some trace element ratios are about constant, e.g. Zr/Nb 5.3 (Fig. 10-B), others are more variable (e.g. Th/U 7-15; Zr/Y 13-26). The differences are compatible with the different ages of the tuffs, determined by comendites.

### *3.3 $^{40}Ar/^{39}Ar$ dating*

All four ages are relatively accurately dated (Renne et al., 1998) and do not yield overlapping ages (Tab. 3). It clearly shows that the four identified units represent four different eruptions in time. The Siakago lower tuff and Ngandurea lower tuff are the oldest of the four. This is also confirmed by their topographic position. Both were strongly weathered for a prolonged period before they were buried by the 6.36 Ma upper tuffs. The deposition of the Gikiiro tuff is about 1.1 Ma younger, followed by the Mavurea tuff, the Siakago upper (not shown in the table) and the Ngandurea upper tuff, the youngest of the four with an age estimate of 6.36 Ma. For more information on the analytical procedure and dating consistency and reliability we refer to Appendix 1.

# Table 3 approx. here

## 4. Discussion

### *4.1 Field observations*

During field work it became clear from the macroscopic tuff characteristics that there are four tuff units. Near Siakago and Ngandurea, two tuffs with similar macroscopic properties overlie each other. There is no obvious relationship between these outcrops and the two localities near Gikiiro and Mavurea.

Based on observed field characteristics, all the tuffs have the properties of distal ash flow deposits. They have many oriented pumice and small rock fragments. They show various degrees of welding, from massive groundmass to basal vitrophyres. Taking the historic 1800 year old Taupo eruption in New Zealand as an analogue of a large-scale pyroclastic deposit (Walker et al., 1981), certain similarities may be observed. At Taupo, pyroclastic deposits are found in a roughly circular area at least 150 km from the central vent and pumice fragments have been observed up to 240 km from the eruptive center (Claessens et al., 2009). Within a 150 km radius of Taupo and up to 1 km above the eruption center, the landscape is covered by pyroclastic deposits. During their eruptions the pantelleritic pyroclastic flows in Kenya only had to overtop the rift valley shoulders. During the Late Miocene there was much less relief as the main rifting phase still had to occur (post Kinangop tuff phase, 3.4 Ma; Baker et al., 1988) and the Aberdares volcano complex (5-6.5 Ma; Baker et al., 1971, p. 205) did not exist yet. This implies that there were no large topographical barriers between the eruption center and the studied location during the Late Miocene. Furthermore, in the Taupo area two types of deposits have been recognized: ignimbrite veneer deposits and valley pond deposits. The thicker ash rich valley pond (tuff) deposits form flat-floored bottom terraces in valleys up to 165 km from the collapsed caldera center. The Taupo tuff deposits at distances > 50 km from the source have very fine textures, vitrophyres and no clear distinguishable banding or structures. These are all properties, which are also valid for our tuff deposits in Kenya. The flat-topped morphology, the underlying gravels, frequent fossil reed imprints or the fine textures, all imply that our tuff deposits are remnants of such pyroclastic valley pond deposits.

The fact that the oldest 8.13 Ma tuff is systematically covered by 6.36 Ma tuffs suggests that there was almost no uplift during the Late Miocene because both tuffs are valley pond deposits. If uplift had occurred between 8.13 and 6.36 Ma, the resulting fluvial incision would have caused the younger tuffs to be at lower topographic positions within an incised valley. As a reference, during the last 1 Ma the Tana river incised about 100 m (Veldkamp et al, 2007). This might also explain why there is no clear relationship between the different tuffs and altitude. Active uplift did occur from the Late Pliocene (Veldkamp et al., 2012) onwards, causing the Tana river to incise and driving erosion of the surrounding landscape. All landscape below 1100 m belongs to this younger incisional phase. As a result, relief inversion positioned the tuffs high up (>1100 m) in the current landscape so that the tuffs have preserved remnants of the Late Miocene topography. Combining all the field evidence suggests that we have found evidence of four different ‘Taupo-like’ eruptions during the Late Miocene in the central sector of the Kenyan Rift.

### *4.2 Geochemistry*

All the analysed tuffs were formed from pantelleritic ash flows. Furthermore, they are highly evolved compositionally, suggesting a mature high-level magma reservoir (Mahood, 1984; Macdonald and Scaillet, 2006; Macdonald, 2012). True pantellerites are uncommon in the Kenyan Rift because Miocene pantellerite centers have been recorded only from northern Kenya (Watkins, 1987; McDougall and Watkins, 1988). However, these are too distant to be directly related to the study area tuffs. Perhaps the nearest compositional analogues in central Kenya come from the Eburru complex at Lake Naivasha (Ren et al., 2006; Fig. 1-A) but are too young to be directly related to the Late Miocene tuffs (<0.45 Ma; Clarke et al., 1990). Nevertheless, it is possible that the eruptive center(s) lay in the Naivasha region, in what Macdonald and Scaillet (2006) termed the central Kenya peralkaline province. The province comprises five young (<1 Ma) volcanic complexes dominated by peralkaline trachytes and rhyolites. It coincides with an area of crustal upwarping known as the Kenya dome, with its maximal topographic height near Lake Nakuru. The dome is apparently in isostatic equilibrium and is supported by the loading of anomalous mantle within the underlying lithosphere (Smith, 1994). It seems possible that this area of anomalous mantle generated the parental magmas (basalts?) and also promoted the Miocene peralkaline magmatism.

In a study of the chemical composition of Kenyan obsidians, Brown et al. (2013) identified one widespread, compositionally homogenous occurrence in an ash flow tuff, the so-called Lukenya Hill group (Fig. 1-A). This rhyolitic obsidian displays a uniform composition from Githumu (40 km south of Nyeri) to Lukenya (10 km west of Machakos) to the western Kenya rift-shoulders along the Mau-Escarpment (165 km to the west), overall covering an area of at least 8750 $km^2$. This area largely overlaps with the geographical projection of the four dated Miocene tuffs. In terms of major elements, it is also very similar to the tuffs, especially the Mavurea tuff (Tab. 2).

Furthermore, within the sedimentary sequence of the Miocene Tugen Hills (Fig. 1-A), a large trachytic ash flow deposit (Deino, pers. comm.), the so-called Mpesida Beds (Chapman and Brook, 1978; Kingston et al., 2002), has a similar $^{40}Ar/^{39}Ar$ age (6.36 Ma) to the Ngandurea tuffs. This might suggest a similar origin, but without geochemical compositional confirmation, no definite correlation can be established.

We have at least one group correlative tuff deposits (Lukenya Hill group) within Kenya, suggesting an even larger geographical spread than that delineated for the 'Pliocene tuffs' by Smith (1994). The 'Pliocene tuffs' were found around the central sector of the Kenyan Rift valley in an area with a radius of ~90 km (Fig. 1-A) it appears that the outcrops of the Late Miocene pantelleritic tuffs have a radius of 150 km (Fig. 1).

What is also striking is that the four tuffs fill a time gap in the magmatic history of central Kenya. In the most recent reconstruction (Macgregor, 2015) is a temporal gap in the volcanism between 8 Ma (end of the phonolitic flood eruptions) and the 5 Ma Kinangop tuffs. It appears that the large-scale, tuff-generating eruptions had already started in the Late Miocene, at around 8 Ma. These first eruptions were very far-reaching and generated pantellerites, indicating that the tuffs originated from shallow magma chambers after extensive magma fractionation histories during the Late Miocene.

### *4.3 Large scale eruptions*

All four tuffs show characteristics of distal ash flow deposits, implying long travel distances. Furthermore, the inferred source area (central sector of the rift system) is 150 km to the west, pointing to four large-scale volcanic eruptions during the Late Miocene. Rhyolitic pyroclastic deposits are highly variable in bulk volume (0.1 to over 1000 km$^3$) and run-out distances (1 to over 100 km) (Freundt et al., 1999). The fact that pyroclastic flows can scale relief of up to 1000 m suggests that topography is not a major factor in determining the distance reached. Legros and Kelfoun (2000) demonstrated for the 86 AD Taupo eruption that a dilute current was responsible for transporting the ignimbrites to their limit. This system property appears to be also valid for our tuff-forming events. This implies that large-scale geometry ignimbrites such as the Miocene tuffs are dilute flow features from eruptions with high discharge rates (10$^2$-10$^3$ Mt/s).

Although varying in detail, the pantelleritic eruptions displayed in Figure 10-B showed broadly similar histories. An initial tall plinian ash column can become gravitationally unstable and collapse (in part or in whole) to form an ash flow. During the initial phase, the ash particles and exsolved gas are capable to reach the stratosphere, where the gases are oxidized to $SO_2$ and form aerosols. Both, ash and aerosols, can be transported laterally for large distances but will eventually be deposited on the Earth's surface. Thus the deposits from peralkaline rhyolitic eruptions have been recorded at great distance from their source center. For example, ash from the relatively small

Green Tuff eruption, Pantelleria (Fig. 10-B), has been recorded as far as the Dodecanese, some 1300 km east of Pantelleria (Margari et al., 2007).

### *4.4 Environmental impact of eruptions*

Given that the Taupo eruptions in New Zealand had a significant environmental impact (Newnham et al., 1999), it is reasonable to infer an environmental signal related to the four large-scale Miocene eruptions. A recent reconstruction of Cenozoic vegetation in East Africa, based on a synthetic pollen diagram of the DSDP 231 marine core from the Gulf of Aden (Bonnefille, 2010), displays an aridity phase (see Fig. 9 in Bonnefille, 2010) between 6.3 and 8.0 Ma, the period during which the four reconstructed large-scale eruptions occurred (Fig. 11). Other studies based on pollen records from northern Kenya (Feakins et al., 2013) and carbon isotopes from herbivore teeth (Uno et al., 2011) show a distinct shift to drier conditions and widespread savannah vegetation during the same period. The most recent compilation of environmental and climate records relevant for Late Cenozoic African paleoenvironmental change (Levin, 2015) gives the most comprehensive overview (Fig. 11). This figure contains relatively high resolution records of charcoal abundance (the fraction of charcoal relative to the sum of pollen, charcoal, and spores) from ODP Site 1081 representing fire activity (Hoetzel et al., 2013) - and the proportion of *Poaceae* grass pollen (from ODP site 1081, 1082, 1085 and DSDP site 231; Bonnefille, 2010; Dupont et al., 2013; Feakins et al., 2013; Hoetzel et al., 2013). Within the range of given temporal uncertainties, the ages of our four tuff events correlate remarkably well with the charcoal and grass pollen records (Fig. 11). It appears that every major volcanic event coincides with a peak in charcoal abundance and they are often followed by an increase in grass pollen. This match may be coincidental but supports our suggestion that the large scale volcanic events may have helped to push the African vegetation stepwise towards more grass dominated vegetation types. Assuming the match is causal the charcoal peaks suggest that we might expect to find more large scale eruptions around 5.0, 5.8 and 6.4 Ma. As a matter of fact there are published Kenyan tuff ages known from 5.8 and 6.4 Ma (Jones and Lippard, 1979), but unfortunately we do not know the extent of these eruptions. It is only speculative, which mechanism caused the apparent correlation, but it suggests an African wide impact of the Late Miocene Kenyan eruptions. The volcanic eruptions seem to have contributed to both variability and instability, which caused not only regional but apparently also continental environmental change. Whether there is a causality between the vegetation change towards more grasslands and the large-scale eruptions remains to be investigated. All four tuffs have some fossilized wood fragments, pointing to the presence of trees in the environment during the ash flow eruption. However, these trees could have been local riparian valley vegetation as the tuffs are preserved only in pre-existing valleys. The eruptions certainly destroyed thousands of square kilometers of the existing ecosystems in central Kenya.

A contributory factor to the environmental effects of the peralkaline magmatism may have been the levels of sulfur emitted during the eruptions. Based on experiments and theoretical calculations, Scaillet and Macdonald (2006) showed that fluid/melt partition coefficients calculated for a pantellerite from Eburru are <50 at 1.5 kbar/800°C and a bulk sulfur content of 1 wt.%. Given their compositional similarities (Figs. 10-A and 10-B), it is not unreasonable to assume that the Kenya tuffs had similar sulfur contents to the Pantellerian magmas. The high solubility of sulfur in peralkaline rhyolitic melts means that it is largely retained in the melt till eruption occurs. Using the Scaillet and Macdonald (2006) results as a basis, Neave et al. (2012) calculated that a relatively small pantelleritic eruption on Pantelleria, the 7 $km^3$ Green Tuff, had a sulfur yield of 80-160 Mt. Without knowledge of the sulfur content of the Miocene magmas, or estimates of the eruptive volumes, similar calculations of sulfur yield cannot be made. However, if the magmas had similar sulfur concentrations to Pantellerian pantellerites (up to 600 ppm; Neave et al., 2012), very significant amounts of sulfur were most likely injected into the atmosphere. Environmental consequences would have included surface temperature decrease, the direct effects of acid rain on the fauna and flora, and acidification of lakes. Recent simulations of similar scale eruptions and the effects of volcanic aerosols on climate forcing, indicate that grass covers recover much faster than forest, potentially leading to a competitive advantage of grass ecosystems (Timmreck et al., 2012). Therefore, we suggest that a series of these eruptions caused significant palaeoenvironmental changes and destroyed the regional vegetation of thousands of square kilometers in central Kenya. Probably grasses preferentially recolonized the extensive tuff-covered areas creating stepwise more extensive savannahs. This may have accelerated the transition of eastern African vegetation from forest towards more open savannah dominated environments, whereas at the same time in non-volcanic western Africa, a forest rich cover of the surface remained (Bonnefille, 2010).

Following the recent theories that lakes have been crucial in hominid evolution (Maslin et al., 2014), the related calderas (lakes) might have been instrumental in this evolution, too. The key component that Maslin et al. (2014) did not include in their theories of environmental control on early human evolution is volcanism. They made a convincing case about the role of climate and tectonics, but did not consider the direct and indirect effects of large volcanic eruptions in destroying and creating environments and lakes.

## 5. Conclusions

In the area south-east of Embu four ash flow tuffs have pantelleritic composition. The four units yield Late Miocene ($^{40}$Ar/ $^{39}$Ar) ages ranging from 6.36 to 8.13 Ma. The tuffs seem to correlate well with one documented large scale tuff deposit (Lukenya Hill group). This is confirmed by the occurrence of large-scale pyroclastic deposits, which possibly originated from a precursor of the central Kenya peralkaline province in the Kenyan rift valley. Our observations imply that the peralkaline volcanic activity had already started in the Miocene. The fact that multiple thick tuff deposits have been preserved up to 150 km away from the inferred eruptive center(s) indicates multi-cyclic supereruptions during the Late Miocene. These eruptions destroyed existing ecosystems, and created new environments, which may have been instrumental in contributing to the increase in savannah areal and human evolution during this period in East Africa.


## Acknowledgements

Alan Deino is thanked for providing more background information about the Mpesida tuffs in the Tugen Hills. Fieldwork was partly supported by the CGIAR Research Program on Climate Change, Agriculture and Food Security (CCAFS). We thank Henry Wichura for useful suggestions and comments on an earlier version of the manuscript.


## References


Baker, B.H., Williams, L.A.J., Miller, J.A., Fitch, F.J., 1971. Sequence and geochronology of the Kenya rift volcanics. Tectonophysics 11, 191-215.

Baker, B.H., Mitchell, J.G., Williams, L.A.J., 1988. Stratigraphy, geochronology and volcano-tectonic evolution of the Kedong–Naivasha–Kinangop region, Gregory Rift Valley, Kenya. Journal of the Geological Society 145, 107-116.

Bear, L.M., 1952. A geological reconnaissance of the area south-east of Embu. Geological Survey of Kenya. Report no 23.

Bonnefille, R., 2010. Cenozoic vegetation, climate changes and hominid evolution in tropical Africa. Global and Planetary Change 72, 390-411.

Brown, F.H., McDougall, I., 2011. Geochronology of the Turkana depression of Northern Kenya and Southern Ethiopia. Evolutionary Anthropology 20, 217-227.

Brown, F.H., Nash, B.P., Fernandez, D.P., Merrick, H.V., Thomas, R.J., 2013. Geochemical composition of source obsidians from Kenya. Journal of Archaeological Science 40, 3233-3251.

Chapman, G.R., Brook, M., 1978. Chronostratigraphy of the Baringo Basin, Kenya. Geological Society Special Publication 6, 207-223.

Claessens, L., Veldkamp, A., ten Broeke, E.M., Vloemans, H., 2009. A Quaternary uplift record for the Auckland region, North Island, New Zealand, based on marine and fluvial terraces. Global and Planetary Change 68, 383-394.

Clarke, M.C.G., Woodhall, D.G., Allen, D., Darling, G., 1990. Geological, volcanological and hydrological controls on the occurrence of geothermal activity in the area surrounding Lake Naivasha, Kenya. British Geological Survey and Kenya Ministry of Energy. Derry and Sons Ltd, Nottingham. 138 pp.

Dupont, L., Rommerskirchen, F., Mollenhauer, G., Schefuss, E., 2013. Miocene to Pliocene changes in South African hydrology and vegetation in relation to the expansion of C4 plants. Earth Planetary Science Letters 375, 408-417.

Fairburn, W. A., 1963. Geology of the North Machakos-Thika Area. Geological Survey of Kenya. Report 59.

Fairburn, W. A., 1966. Geology of the Fort Hall Area. Geological Survey of Kenya. Report 73.

Feakins, S.J., Levin, N.E., Liddy, H.M., Sieracki, A., Eglinton, T.I., Bonnefille, R., 2013. Northeast African vegetation change over 12 million years. Geology 41, 295-298.

Freundt, A., Wilson, C. J. N., Carey, S. N., 1999. Ignimbrites and Block-And-Ash Flow Deposits. In: Sigurdsson, H. (Ed.), Encyclopedia of Volcanoes. Academic Press, pp. 581-599.

Hoetzel, S., Dupont, L., Schefuss, E., Rommerskirchen, F., Wefer, G., 2013. The role of fire in Miocene to Pliocene C4 grassland and ecosystem evolution. Nature Geoscience 6, 1027-1030.

Jarvis A., Reuter, H.I., Nelson, A., Guevara, E., 2008. Hole-filled seamless SRTM data V4, International Centre for Tropical Agriculture (CIAT), available from http://srtm.csi.cgiar.org.

Jones, W.B., Lippard, S.J., 1979. New age determinations and the geology of the Kenya rift – Kavirondo Rift junction, West Kenya. J. Geol. Soc. Lond. 136, 693-704.

Kingston, J.D., Fine Jacobs, B., Hill, A., Deino, A., 2002. Stratigraphy, age and environments of the late Miocene Mpesida Beds, Tugen Hills, Kenya. Journal of Human Evolution 42, 95-116.

Koppers, A.A.P., 2002. ArArCALC- software for 40Ar/39Ar age calculations. Computers and Geoscience 28, 605 – 619.

Leat, P.T., 1991. Volcanological development of the Nakuru area of the Kenya rift valley. Journal of African Earth Sciences 13, 483-498.

Le Bas, M.J., Le Maitre, L.W., Woolley, A.R., 1992. The construction of the Total Alkali-Silica Chemical Classification of Volcanic Rocks. Mineralogy and Petrology 46, 1-22.

Legros, F., Kelfoun, K., 2000. On the ability of pyroclastic flows to scale topographical obstacles. Journal of Volcanology and Geothermal Research 98, 235-241.

Levin, N.E., 2015. Environment and Climate of Early Human Evolution. Annual Review of Earth and Planetary Sciences 432, 405-429.

Macdonald, R., 1974. Nomenclature and petrochemistry of the peralkaline oversaturated extrusive rocks. Bulletin Volcanologique 38, 498-516.

Macdonald, R., 2012. Evolution of peralkaline silicic complexes: Lessons from the extrusive rocks. Lithos 152, 11-22.

Macdonald, R., 2003. Magmatism of the Kenya Rift Valley: a review. Transactions of the Royal Society of Edinburgh: Earth Sciences 93, 239-253. J. Petrology 28, 979-1008.

Macdonald, R., Davies, G.R., Bliss, C.M., Leat, P.T., Bailey, D.K., Smith, R.L., 1987. Geochemistry of High-silica Peralkaline Rhyolites, Naivasha, Kenya Rift Valley.

Macdonald, R., Bagiński, B., Leat, P.T., White, J.C., Dzierżanowski, P., 2011. Mineral stability in peralkaline silicic rocks: insights from trachytes of the Menengai volcano, Kenya Rift Valley. Lithos 125, 553-568.

Macdonald, R., Scaillet, B., 2006. The central Kenya peralkaline province: Insights into the evolution of peralkaline salic magmas. Lithos 91, 59-73.

Macgregor, D., 2015. History of the development of the East African Rift System: a series of interpreted maps through time. Journal of African Earth Sciences 101, 232-252.

Mahood, G.A., 1984. Pyroclastic rocks and calderas associated with strongly peralkaline magmatism. Journal of Geophysical Research 89, 8540-8552.

Margari, V., Pyle, D.M., Bryant, C., Gibbard, P.L., 2007. Mediterranean tephra stratigraphy revisited: results from a long terrestrial sequence on Lesvos Island, Greece. Journal of Volcanology and Geothermal Research 163, 34-54.

Maslin, M.A., Brierley, C.M., Milner, A.M., Shultz, S., Trauth, M.H., Wilson, K.E., 2014. East African climate pulses and early human evolution. Quaternary Science Reviews 101, 1-17.

McCall, G.J.H., 1967. Geology of the Nakuru-Thomson's Falls-Lake Hannington area. Geological Survey of Kenya. Report 78.

McDougall I., Watkins, R. T., 1988. Potassium–argon ages of volcanic rocks from northeast of Lake Turkana, northern Kenya. Geological Magazine 125, 15-23.

Middlemost, E.A.K., 1989. Iron oxidation ratios, norms and the classification of volcanic rocks. Chemical Geology 77, 19-26.

Neave, D.A., Fabbro, G., Herd, R.A., Petrone, C.M., Edmonds, M., 2012. Melting, differentiation and degassing at the Pantelleria volcano, Italy. Journal of Petrology 53, 637-663.

Newnham, R.M., Lowe, D.J., Williams, P.W., 1999. Quaternary environmental change in New Zealand: A review. Progress in Physical Geography 23, 567-610.

Ren, M., Anthony, E.Y., Omenda, P.A., White, J.C., Macdonald, R., Bailey, D.K., 2006. Application of the QUILF thermobarometer to the peralkaline trachytes and pantellerites of the Eburru volcanic complex, East African Rift, Kenya. Lithos 91, 109-124.

Renne P.R., Karner D.B., Ludwig K.R., 1998. Radioisotope dating - Absolute ages aren't exactly. Science 282 (5395), 1840-1841.

Reuter, H.I., Nelson, A., Jarvis, A., 2007. An evaluation of void filling interpolation methods for SRTM data. International Journal of Geographic Information Science 21, 983-1008.

Scaillet, B., Macdonald, R., 2006. Experimental and thermodynamic constraints on the sulphur yield of peralkaline and metaluminous silicic flood eruptions. Journal of Petrology 47, 1413-1437.

Schneider, B., Kuiper, K., Postma, O., Wijbrans, J., 2009. $^{40}Ar/^{39}Ar$ geochronology using a quadrupole mass spectrometer. Quaternary Geochronology 4, 508-516,

Schoorl, J.M, Veldkamp, A., Claessens, L., van Gorp, W., Wijbrans, J.R., 2014. Edifice growth and collapse of the Pliocene Mt. Kenya: evidence of large scale debris avalanches on a high altitude glaciated volcano. Global and Planetary Change 123, 44-54.

Smith, M., 1994. Stratigraphic and structural constraints on mechanism of active rifting in the Gregory rift, Kenya. Tectonophysics 236, 3-22.

Timmreck, C., Graf, H.-F., Zanchettin, D., Hagemann, S., Kleinen, T., Krüger, K., 2012. Climate response to the Toba super-eruption: Regional changes. Quaternary International 258, 30-44.

Uno, K.T., Cerling, T.E., Harris, J.M., Kunimatsu, Y., Leakey, M.G., Nakatsukasa, M., Nakaya, H., 2011. Late Miocene to Pliocene carbon isotope record of differential diet change among East African herbivores. Proc. Natl. Acad. Sci. 108, 6509–6514.

van Gorp, W., Veldkamp, A., Temme, A.J.A.M., Maddy, D., Demir, T., van der Schriek, T., Reimann, T., Wallinga, J., Wijbrans, J., Schoorl, J.M., 2013. Fluvial response to Holocene volcanic damming and breaching in the Gediz and Geren rivers, western Turkey. Geomorphology 201, 430-448.

Veldkamp, A., Visser, P.W., 1992. Erosion surfaces in the Chuka-South area, central Kenya. Zeitschrift fur Geomorphologie, Supplementband. Volume 84, 147-158.

Veldkamp, A., Buis, E., Wijbrans, J.R., Olago, D.O., Boshoven, E.H., Marée, M., van den Berg van Saparoea, R.M., 2007. Late Cenozoic fluvial dynamics of the River Tana, Kenya, an uplift dominated record. Quaternary Science Reviews 26, 2897-2912.

Veldkamp, A., Schoorl, J.M., Wijbrans, J.R., Claessens, L., 2012. Mount Kenya volcanic activity and the Late Cenozoic landscape reorganisation in the upper Tana fluvial system. Geomorphology 145–146, 19-31.

Walker, G.P.L., Wilson, C.J.N., Froggatt, P.C., 1981. An ignimbrite veneer deposit: the trail-marker of a pyroclastic flow. Journal for Volcanology and Geothermal Research 9, 409-421.

Watkins, J.L., 1987. Geology of Kubi Algi and Derati mountains, pantellerite bodies of Miocene age from the northern part of the Kenyan Rift Valley. African Earth Sciences 6, 603-616.

Wichura, H., Jacobs, L.L., Lin, A., Polcyn, M.J., Manthi, F.K., Winkler, D.A., Strecker, M.R., Clemens, M., 2015. A 17-My-old whale constrains onset of uplift and climate change in east Africa. Proc. Natl. Acad. Sci. 112, 3910-3915.

Wijbrans, J., Schneider, B., Kuiper, K., Calvari, S., Branca, S., De Beni, E., Norini, G., Corsaro, R.A., Miraglia, L., 2011. $^{40}Ar/^{39}Ar$ geochronology of Holocene basalts; examples from Stromboli, Italy. Quaternary Geochronology 6, 223-232.

## Figure captions

Figure 1: Geological setting. (A) Location of study area and other localities within Kenya. (Nak = Nakuru; Nai = Naivasha; Sus = Suswa; Nbi = Nairobi; Mac = Machakos; Emb = Embu). (B) Simplified regional geology map of the study area (after Bear, 1952) with the locations and ages of the tuffs. Note the depressions in the VDA deposit as mapped in Schoorl et al. (2014). Coordinates in UTM (zone 37).

Figure 2: Schematic cross-sections of the investigated four tuff sites: Siakago tuffs (site A), Ngandurea tuffs (site B), Gikiiro tuff (site C), and Mavurea tuff (site D). Abbreviations: a.s.l. (above sea level).

Figure 3: Photographs of the Siakago upper tuff. (A) the General outcrop with thick soil development. (B) A close-up of the tuff. Note pale gray color and flattened pumice fragments. (C) The basal vitrophyre of the tuff.

Figure 4: Photographs of the Siakago lower tuff. (A) The general outcrop. Soil development is less due to truncation in slope position. (B) A close-up of the lower tuff with rounded dark vesicular fragments in a dark grey groundmass.

Figure 5: Photographs of the Ngandurea upper tuff. (A) General outcrop with deep soil development. (B) A close-up of the tuff. Note pale gray color and flattened pumice fragments. (C) The thick basal vitrophyre of the tuff.

Figure 6: More photographs of the Ngandurea upper tuff. (A) Vitric welded base of Ngandurea upper tuff, note the parallel orientation of the vesicals. (B) Fossil wood imprint in tuff.

Figure 7: Photographs of the Ngandurea lower tuff. (A) General outcrop. Soil development is less due to quarrying and slope position. Note the change in color from dark grey to more reddish colors from bottom to top. (B) A close-up of lower tuff with rounded dark vesicular fragments in a dark grey groundmass. (C) Same tuff but due to weathering a more reddish groundmass color.

Figure 8: Photographs of the Gikiiro tuff. (A) Overview of the Gikiiro tuff underlying Kari phonolite flow. The palaeosol in between has greyish hydromorphic features with murram ($Fe_2O_3$ iron-sesquioxide). (B) A close-up of the basal properties with many rounded pumice fragments. (C) A close-up of the greyish groundmass with no distinctive features.

Figure 9: Photographs of the Mavurea upper tuff. (A) An overview of the upper outcrops. (B) A close-up of the tuff with many small pumice and other inclusions. (C) The basal vitrophyre of the Mavurea tuff.

Figure 10: Compositional comparison of tuffs from this study with others from the literature. (A) Classification scheme for peralkaline salic rocks of Macdonald (1974). The Miocene tuffs are pantellerites, closely similar to the type pantellerites from Pantelleria, Italy and to obsidians from the Lukenya Hill Group (Brown et al., 2013). Generalized compositional trends for Pantelleria and Eburru are from Macdonald et al. (2011). FeO* all Fe calculated as $Fe^{2+}$.

(B) Zr-Nb plots of peralkaline ignimbrite units, showing the generalized compositional variation in the pre-eruptive magma chambers and the estimated volumes of each unit, in $km^3$. Also shown are data from this study (G, Giikiro; M, Mavurea; NU, Ngandurea upper; SL, Siakoga lower; Tab. 2) and the Lukenya Hill tuff (LH, dashed field; Brown et al., 2013). Menengai, Kenya, first ash flow tuff; Green tuff, Pantelleria, Italy; Gran Canaria, ignimbrite A; Gomez tuff, Mexico; Fantale tuff, Ethiopia; Tala tuff, Mexico. Modified from Macdonald (2012).

Figure 11: A compilation of environmental and climate records relevant for Late Cenozoic African paleoenvironmental change from Levin (2015). The source records are from the Atlantic Ocean off the western coast of Africa (ODP 1081, 1082, and 1085) and the Gulf of Aden (DSDP 231). These graphs display relatively high resolution records of charcoal abundance (the fraction of charcoal relative to the sum of pollen, charcoal, and spores) from ODP Site 1081 representing fire activity (Hoetzel et al. 2013), and the proportion of *Poaceae* grass pollen (from ODP site 1081, 1082, 1085; Bonnefille (2010); Dupont et al. (2013); Feakins et al. (2013); Hoetzel et al. (2013)). Red dashed lines are the dated tuffs of this study (G, Giikiro; M, Mavurea; NU, Ngandurea upper; SL, Siakoga lower; Tab. 3). Blue dashed lines are other published Kenyan tuff ages (Jones and Lippard, 1979).

Table 1. Site locations and descriptions

| Site | Name location | UTM coordinates (UTM zone 37) | Description of lithology and structures |
|---|---|---|---|
| A | Siakago upper tuff | 0349260-9938102 | • massive pale greyish homogeneous with weak columnar jointing (Fig. 3.A)<br>• Fe and Mn staining on the rock surfaces<br>• numerous parallel oriented flattened whitish pumice fragments and an oriented vesicular structure<br>• locally imprints of reed<br>• total thickness is about 5 m<br>• 0.8 m thick massive basal vitrophyre at the base<br>• resemblance to the Ngandurea upper tuff<br>• 1-2 m thick red soil (Ferralsol) developed on top (Fig. 3.A) |
| | Siakago lower tuff | 0349267-9938089 | • exposed as light grey massive columnar tuff outcrop at least 5 m thick<br>• homogenous and massive<br>• no orientation in the pumice fragments<br>• minor small pumice and vegetation imprint fragments (reed and wood)<br>• frequently dark vesicular black and semi-rounded lithic fragments<br>• macroscopic sanidines feldspars but no basal obsidian glass<br>• dated sample location is 0349179-9938482 (1147 m)<br>• strongly resemblance to the Ngandurea lower tuff<br>• upper 2 m is weathered into dark reddish soil (Fig. 4.A)<br>• sometimes well-sorted greenish fluvial sand at the base |
| B | Ngandurea upper tuff | 0343366-9922539 | • massive pale-grey homogeneous tuff with weak columnar jointing<br>• Fe and Mn staining on the rock surfaces (Fig. 5)<br>• few inclusions of foreign material embedded in an irregularly greyish<br>stained groundmass carrying numerous microlites |

| | | | |
|---|---|---|---|
| | | | • clearly oriented compressed pumice fragments (Fig. 5.B)<br>• occasionally reed and wood imprints in an oriented vesicular structure (Fig. 6.B)<br>• resemblance to the Siakago upper tuff<br>• 1-2 m thick red soil (Ferralsol) developed on top (see Fig. 5.A) |
| | Ngandurea upper tuff base | 0343366-9922539 | • 1 m thick basal vitrophyre characterized by clear orientation of compressed and flattened pumice fragments (both in greyish tuff as in vitrified base; see Figs. 5.B & 5.C) |
| | Ngandurea lower tuff | 0343463-9922529 | • total observed thickness is 6-8 m<br>• top is reddish due to weathering; lower in profile the color changes to a pale yellowish grey<br>• tuff is homogenous massive light grey<br>• no orientation in the pumice fragments<br>• only a few small rounded pumice and vegetation imprint fragments (reed and wood)<br>• frequently dark vesicular black lithic fragments in the fragment are semi-rounded<br>• high amount of sanidine feldspars but no obsidian glass<br>• tuff sequence is overlain by 1 m of solid obsidian (at 1188 m)<br>• strong resemblance to the Siakago lower tuff<br>• upper 3 m is weathered in reddish/pinkish grey colors (Fig. 7.A) |
| C | Gikiiro tuff | 0349559-9927086 | • Kari Phonolite overlying a 0.4 m thick sandy palaeosol (with hydromorphic features) in slope material developed on top of the tuff.<br>• tuff is massive greyish with no clear orientations and poor in lithic fragments<br>• coarse rounded pumice rich unit at the base<br>• no obsidian glass<br>• Maximum thickness is 5 m (Fig. 8) |
| D | Mavurea tuff top | 0352002-9917711 | • sandy reddish soil (30 cm) followed by 70 cm “murram” (laterite)<br>• tuff is weathered along cracks and cemented by ironstone in root channels<br>• homogenous massive light grey<br>• no orientation in the pumice fragments |

| | | | |
|---|---|---|---|
| | | | • rarely small angular pumice and vegetation imprint fragments (reed and small wood) fragments<br>• only a few rounded small fragments as inclusions (Fig. 9.B) |
| | Mavurea tuff base | 0351842-9918084 | • ~ 1 m massive black vitrophyre (see Fig. 9.C) |

Table 2. Geochemical composition of the four tuffs (groundmass) FUS-ICP.

| | Site A: Siakago lower tuff | Site B: Ngandurea upper tuff | Site C: Gikiiro tuff | Site D: Mavurea tuff |
|---|---|---|---|---|
| wt.% | | | | |
| $SiO_2$ | 66,55 | 68,32 | 66,88 | 69,36 |
| $TiO_2$ | 0,54 | 0,56 | 0,56 | 0,47 |
| $Al_2O_3$ | 10,01 | 9,42 | 9,57 | 8,64 |
| FeO* | 8,98 | 8,10 | 7,55 | 8,07 |
| MnO | 0,18 | 0,27 | 0,28 | 0,25 |
| MgO | 0,17 | 0,25 | 0,52 | 0,12 |
| CaO | 0,57 | 0,53 | 0,63 | 0,49 |
| $Na_2O$ | 3,75 | 4,31 | 4,68 | 4,13 |
| $K_2O$ | 3,56 | 4,22 | 4,09 | 4,33 |
| $P_2O_5$ | 0,04 | 0,05 | 0,05 | 0,03 |
| Total | 94,35 | 96,03 | 94,81 | 95,89 |
| | | | | |
| ppm | | | | |
| Ba | 155 | 167 | 331 | 115 |
| Sr | 37 | 24 | 48 | 28 |
| Rb | 75 | 196 | 170 | 218 |
| Y | 71 | 110 | 85 | 88 |
| Zr | 1875 | 1433 | 1241 | 1623 |
| Hf | 42,1 | 34,1 | 29,5 | 37,7 |
| Nb | 355 | 270 | 235 | 302 |
| Ta | 21,8 | 18 | 15,1 | 19,4 |
| Zn | 360 | 410 | 430 | 430 |
| Ga | 46 | 42 | 41 | 41 |
| Th | 47,1 | 37,4 | 32,3 | 43,5 |
| U | 6,5 | 2,7 | 2,1 | 4,8 |
| La | 177 | 306 | 194 | 223 |
| Ce | 340 | 305 | 371 | 301 |
| Pr | 35,8 | 61,1 | 42,3 | 48,7 |
| Nd | 125 | 211 | 150 | 164 |
| Sm | 22,2 | 36,2 | 28,2 | 27,5 |
| Eu | 2,99 | 5,04 | 4,18 | 3,8 |
| Gd | 17,4 | 27,3 | 22,6 | 18,9 |

| | | | | |
|---|---|---|---|---|
| Tb | 2,6 | 4,2 | 3,3 | 3,1 |
| Dy | 14,4 | 21,5 | 17,8 | 17,8 |
| Ho | 2,6 | 4 | 3,2 | 3,5 |
| Er | 2,6 | 4 | 3,2 | 3,5 |
| Tm | 1,08 | 1,57 | 1,29 | 1,7 |
| Yb | 6,9 | 10,1 | 8,3 | 11,4 |
| Lu | 1,12 | 1,68 | 1,38 | 1,86 |

$FeO^*$ all Fe calculated as $Fe^{2+}$

| *CIPW norms* (oxidation ratios after Middlemost, 1989) | | | | |
|---|---|---|---|---|
| q | 28,3 | 26,1 | 24,2 | 29,9 |
| or | 22,2 | 25,9 | 25,4 | 26,6 |
| ab | 33,4 | 25,9 | 27,8 | 21,1 |
| ac | 0,1 | 9 | 8,5 | 9 |
| ns | | 0,4 | 1 | 1,2 |
| di | 2,4 | 2,1 | 2,6 | 2,1 |
| hy | 7,4 | 9,4 | 9,3 | 9,1 |
| il | 1,1 | 1,1 | 1,1 | 0,9 |
| mt | 5,1 | - | - | - |
| ap | 0,1 | 0,1 | 0,1 | 0,1 |

Table 3. $^{40}Ar/^{39}Ar$ dating of the four tuffs.

| Site and tuff | UTM coordinates (UTM zone 37) | **$^{40}Ar/^{39}Ar$ age (Ma)** |
|---|---|---|
| Site A: Siakago lower tuff | 349179-9938482 | **8.13 ± 0.08** |
| Site B: Ngandurea upper tuff | 343608-9924886 | **6.36 ± 0.03** |
| Site C: Gikiiro tuff | 349525-9926913 | **7.03 ± 0.05** |
| Site D: Mavurea tuff | 352084-9917770 | **6.88 ± 0.04** |

Figure 1.

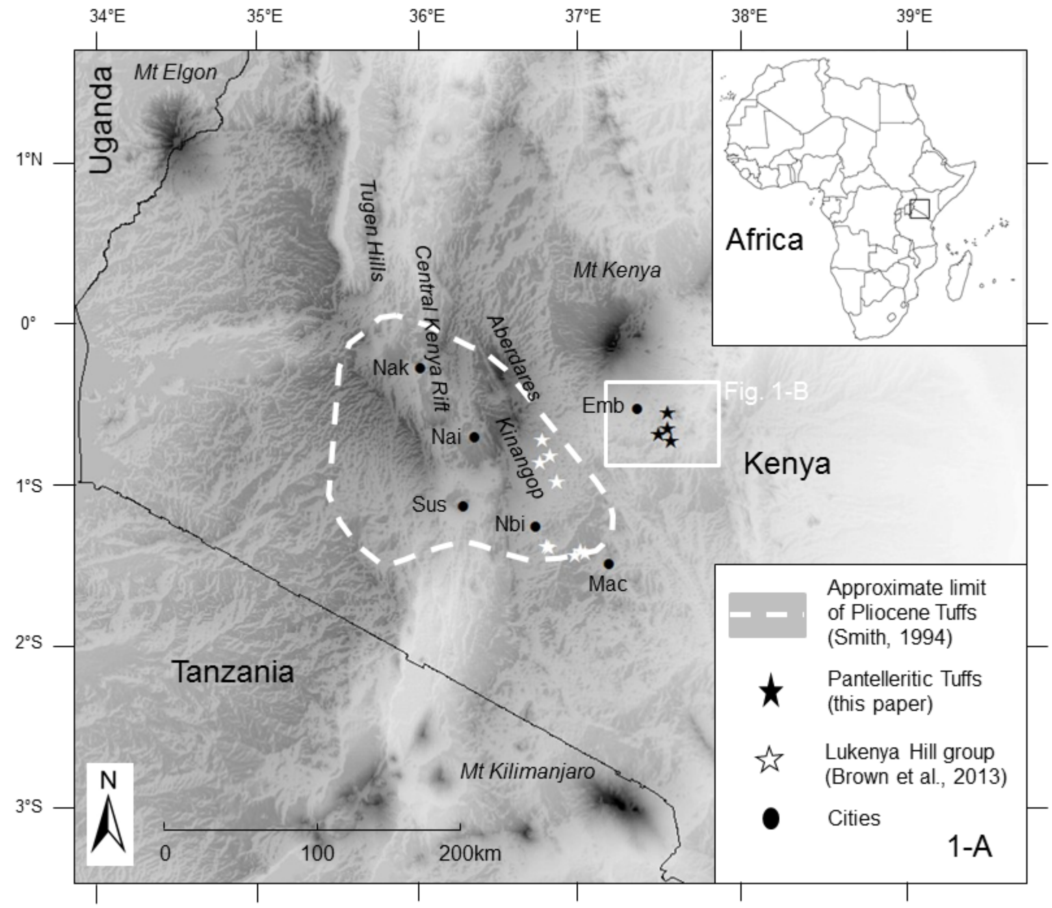
34°E
35°E
36°E
37°E
38°E
39°E
1°N
0°
1°S
2°S
3°S
Uganda
Mt Elgon
Tugen Hills
Central Kenya Rift
Aberdares
Mt Kenya
Kinangop
Nak
Nai
Sus
Nbi
Emb
Mac
Fig. 1-B
Kenya
Africa
Tanzania
Mt Kilimanjaro
N
0
100
200km
Approximate limit of Pliocene Tuffs (Smith, 1994)
Pantelleritic Tuffs (this paper)
Lukenya Hill group (Brown et al., 2013)
Cities
1-A

600

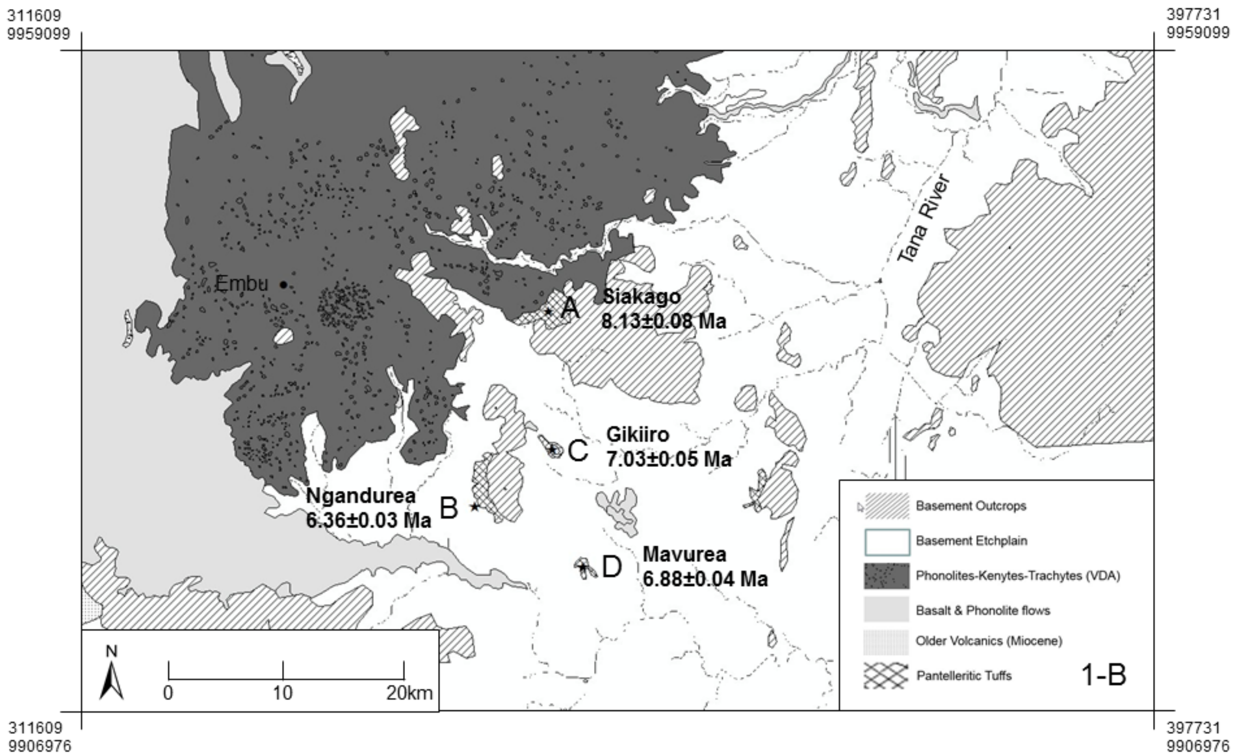
311609
9959099
397731
9959099
Embu
Siakago
8.13±0.08 Ma
A
Tana River
Gikiiro
7.03±0.05 Ma
C
Ngandurea
6.36±0.03 Ma
B
Mavurea
6.88±0.04 Ma
D
Basement Outcrops
Basement Etchplain
Phonolites-Kenytes-Trachytes (VDA)
Basalt & Phonolite flows
Older Volcanics (Miocene)
Pantelleritic Tuffs
1-B
N
0
10
20km
311609
9906976
397731
9906976

Figure 2.

**Site A: 1 km N-S cross-section**

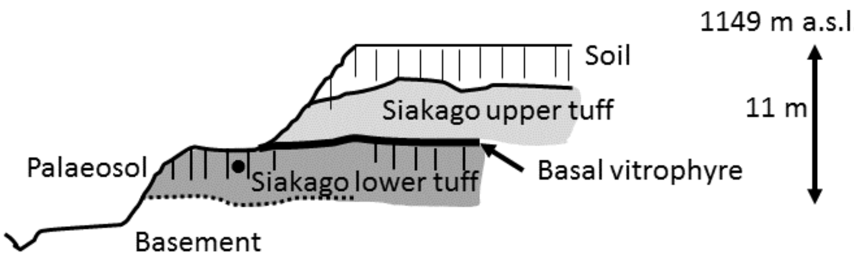


**Site B: 3 km N-S cross-section**

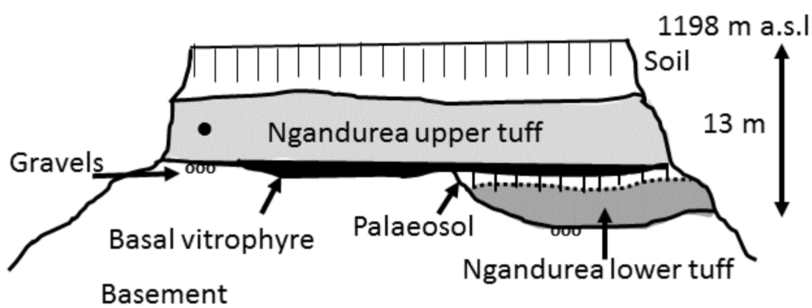

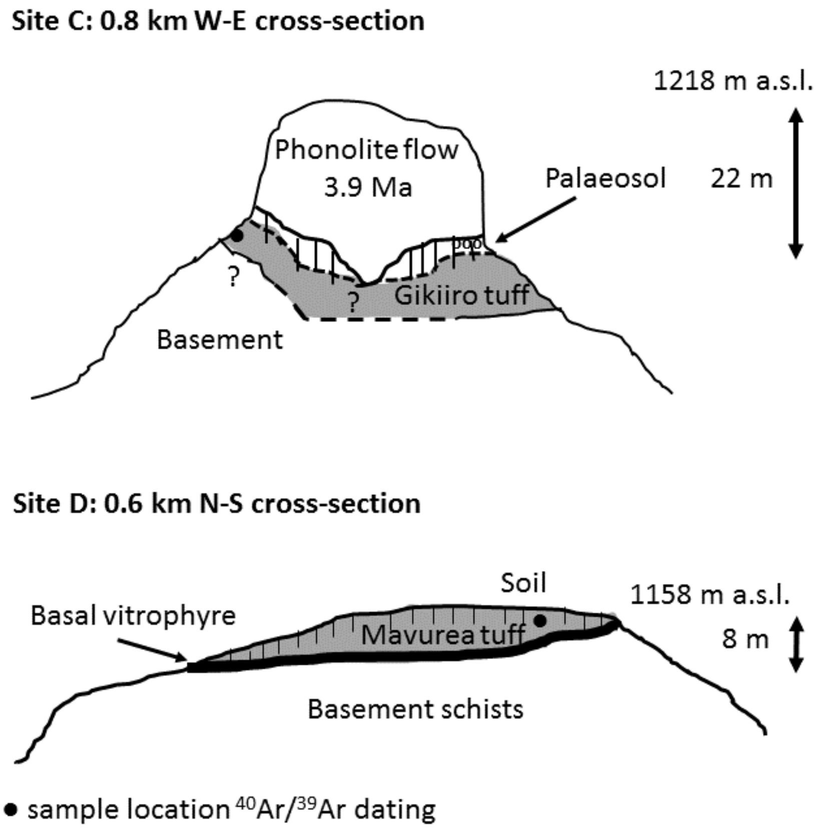
Site C: 0.8 km W-E cross-section
1218 m a.s.l.
Phonolite flow
3.9 Ma
Palaeosol
22 m
?
?
Gikiiro tuff
Basement
Site D: 0.6 km N-S cross-section
Soil
1158 m a.s.l.
Basal vitrophyre
Mavurea tuff
8 m
Basement schists
● sample location $^{40}Ar/^{39}Ar$ dating

Figure 3.

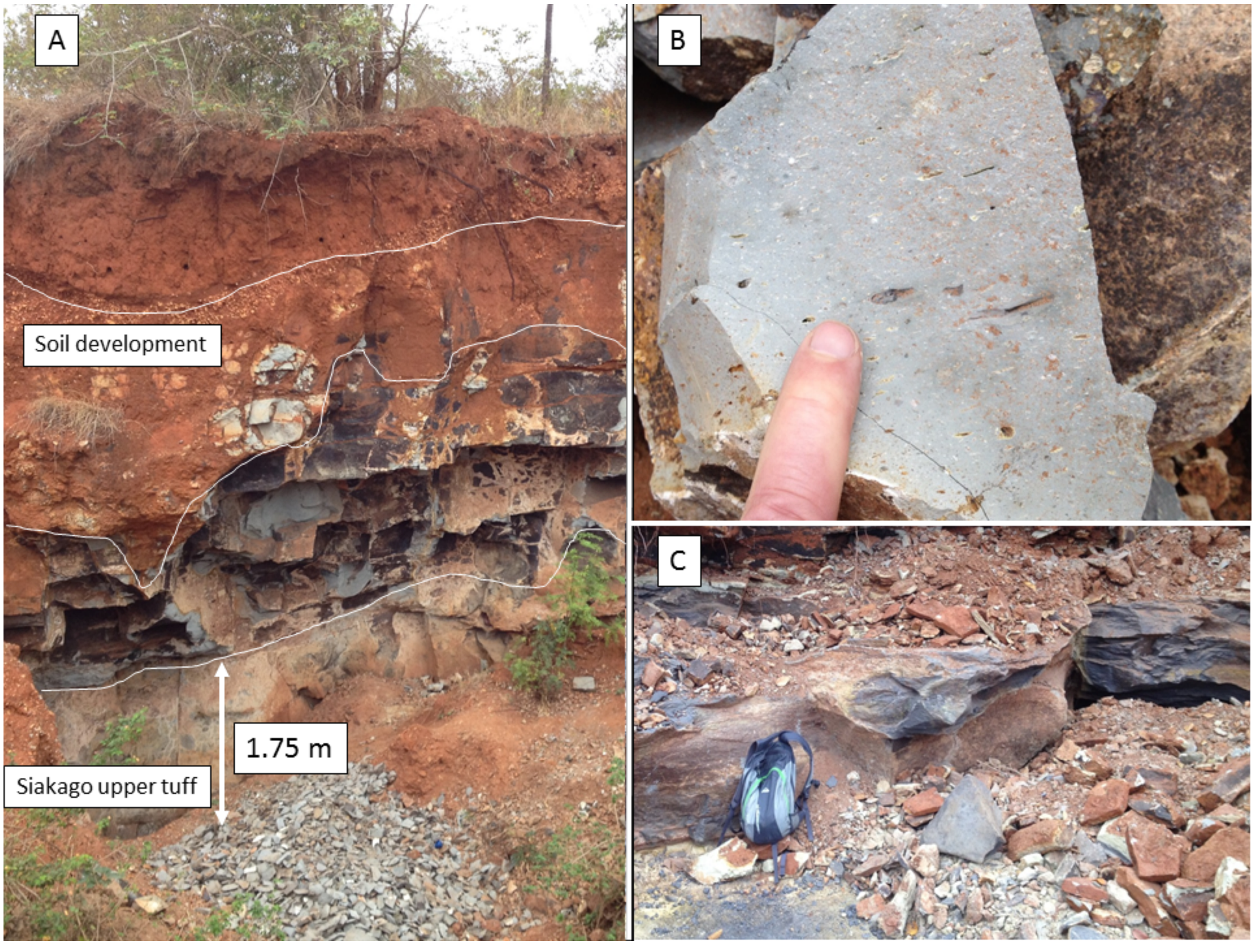


Figure 4.

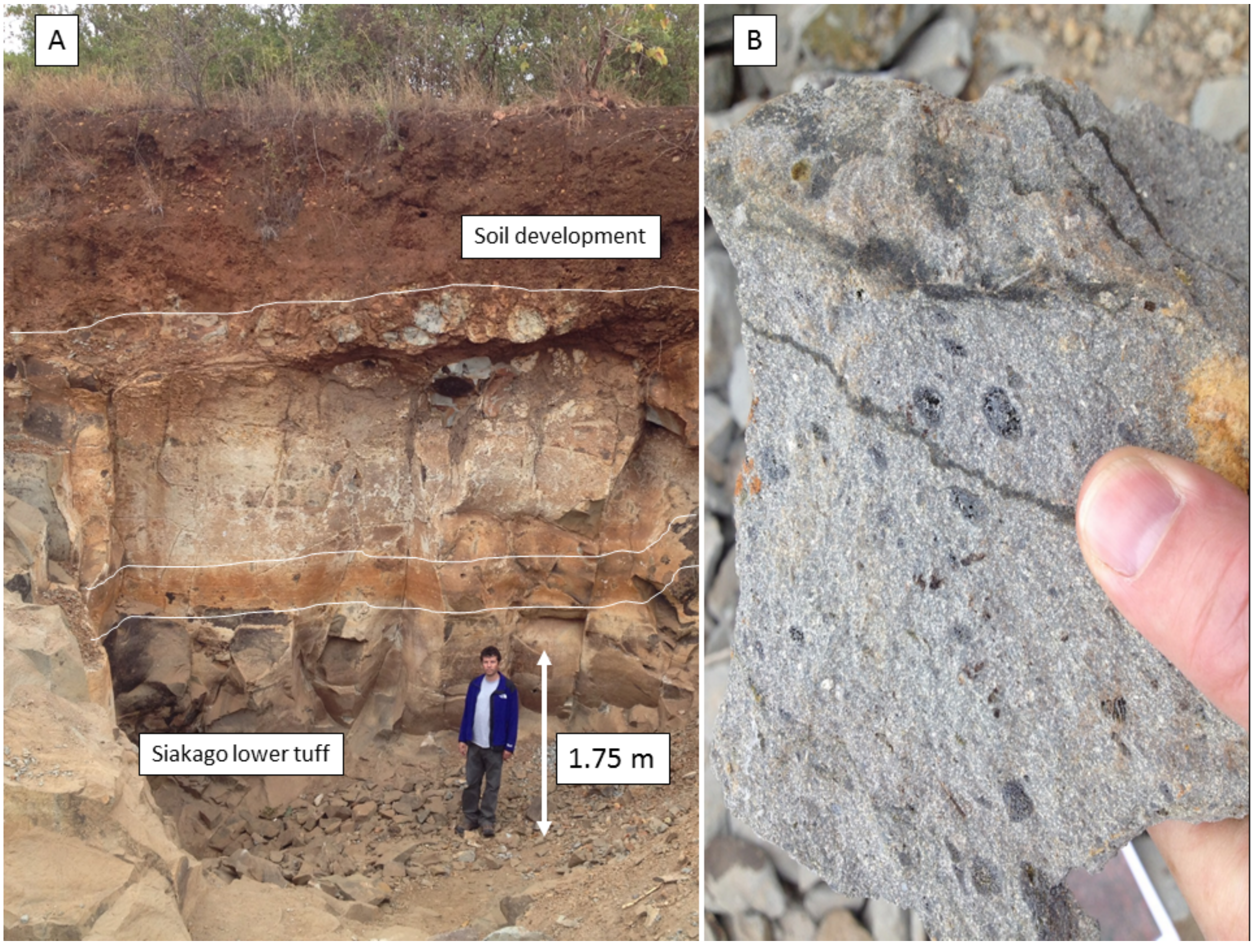


Figure 5.

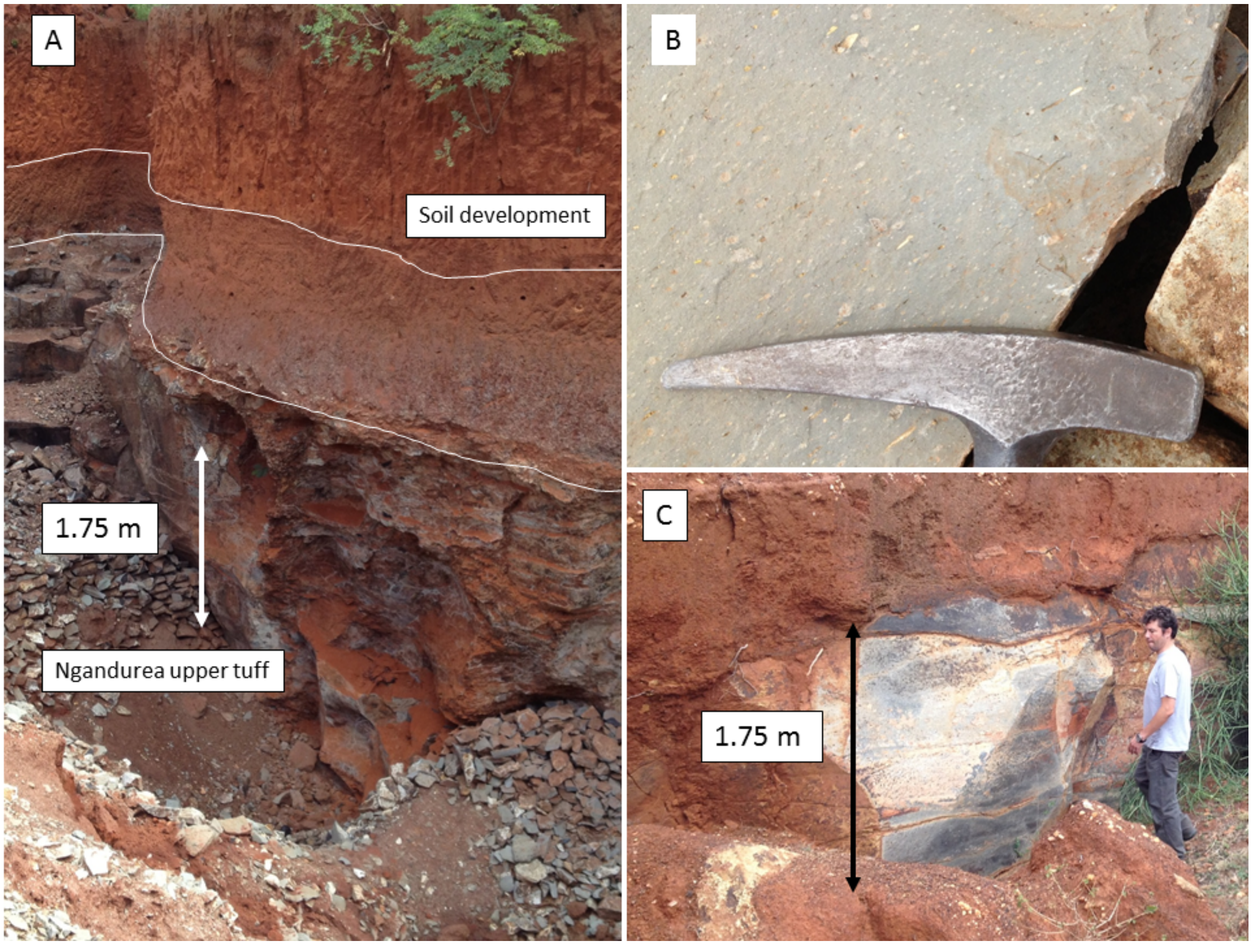


Figure 6.


Figure 7.

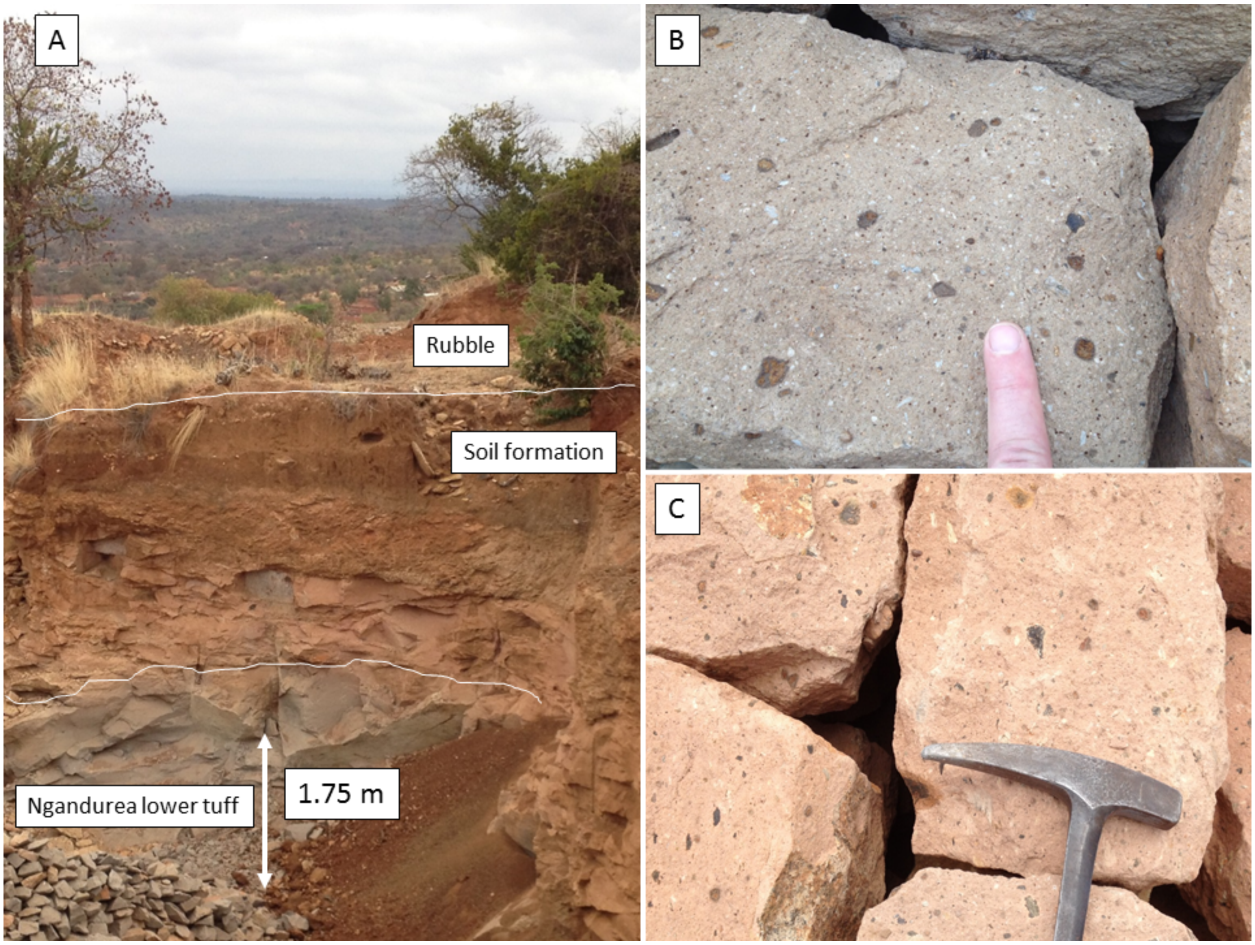


Figure 8.


Figure 9.

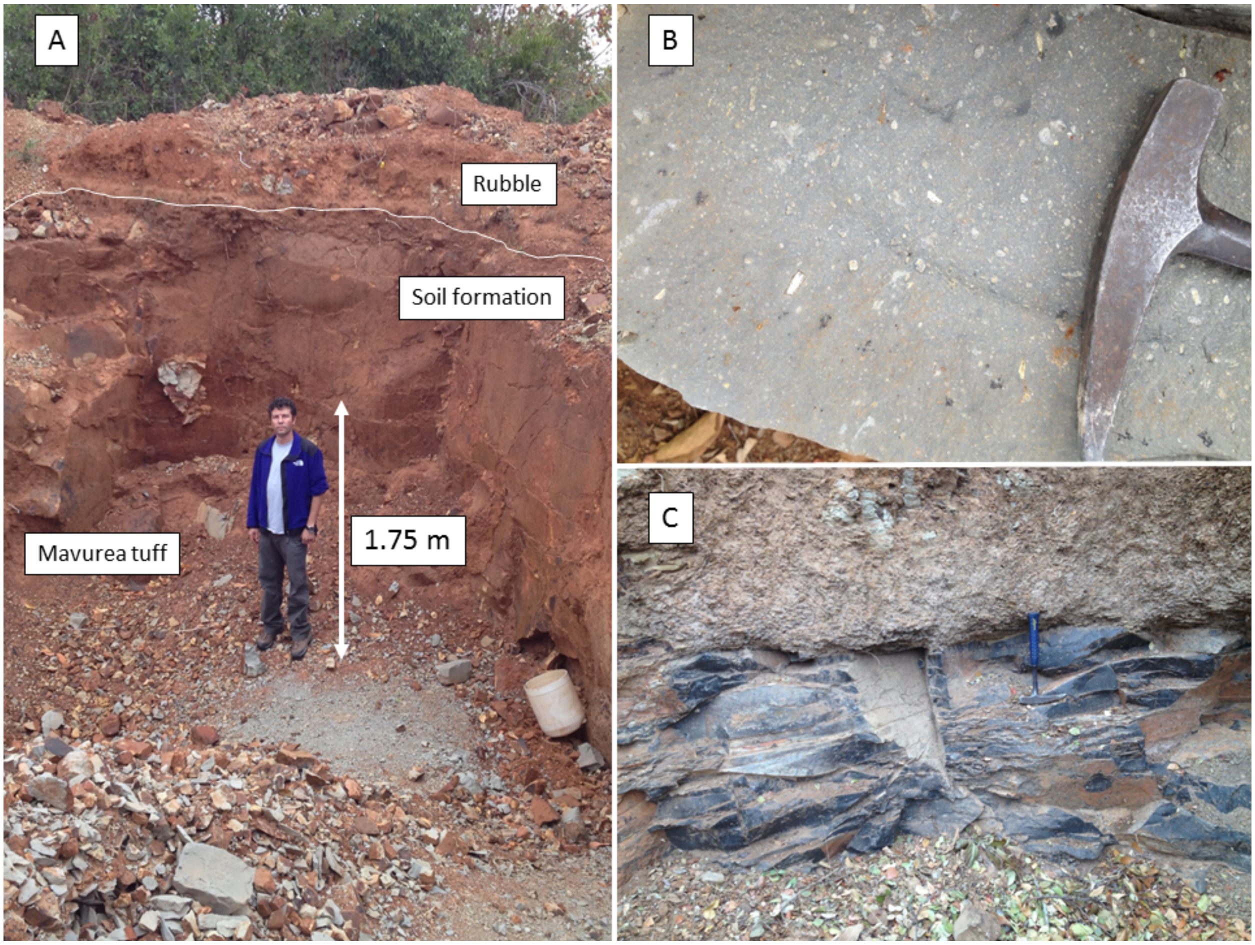


Figure 10-A.

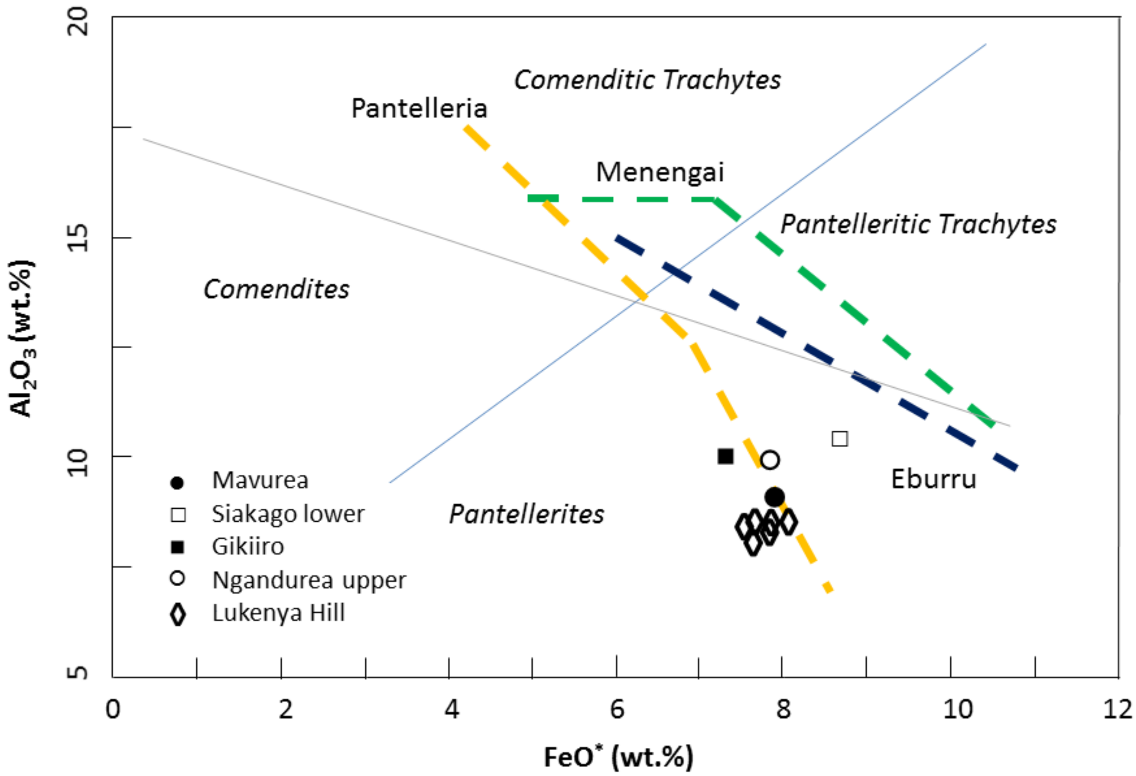
Comenditic Trachytes
Pantelleria
Menengai
Pantelleritic Trachytes
Comendites
Eburru
Pantellerites
Mavurea
Siakago lower
Gikiiro
Ngandurea upper
Lukenya Hill
$Al_2O_3$ (wt.%)
$FeO^*$ (wt.%)
5
10
15
20
0
2
4
6
8
10
12

Figure 10-B.

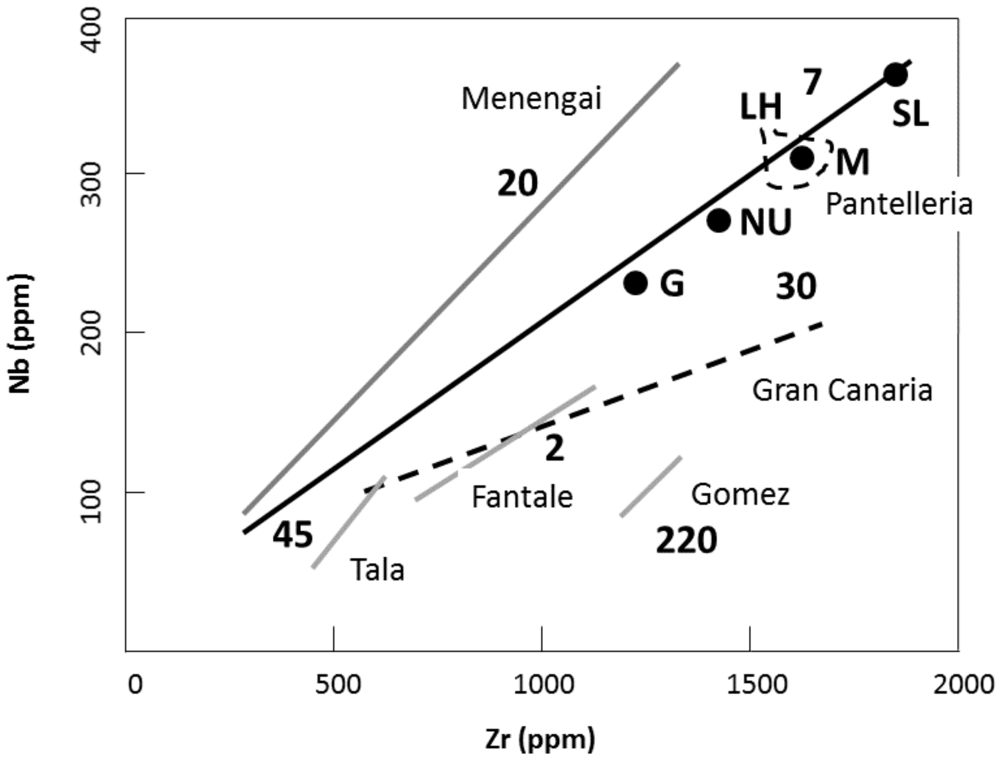
Menengai
20
LH
7
SL
M
Pantelleria
NU
G
30
Gran Canaria
2
Fantale
Gomez
45
220
Tala
400
300
200
100
Nb (ppm)
0
500
1000
1500
2000
Zr (ppm)

Figure 11.

633

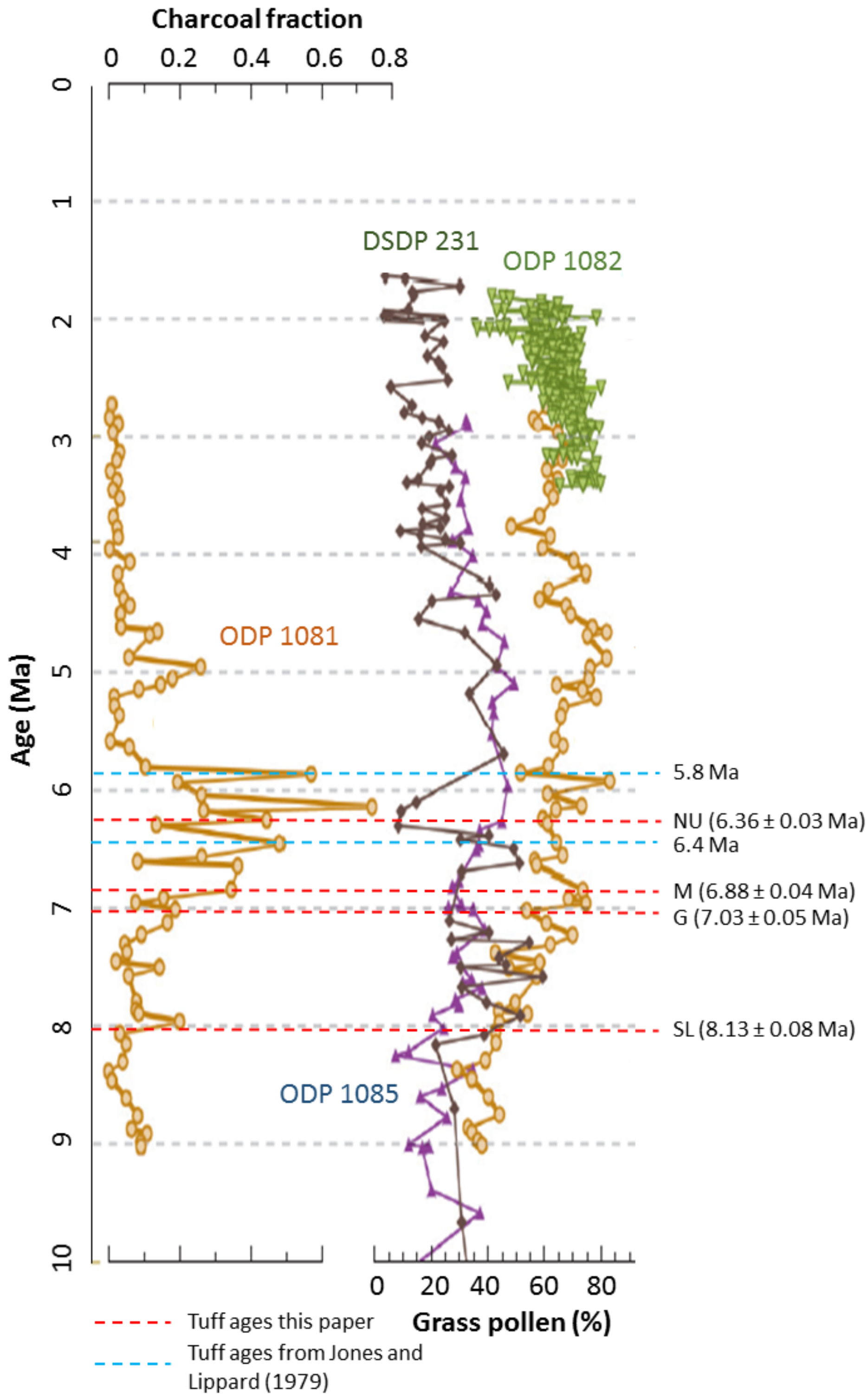

Charcoal fraction
0
0.2
0.4
0.6
0.8
Age (Ma)
0
1
2
3
4
5
6
7
8
9
10
DSDP 231
ODP 1082
ODP 1081
ODP 1085
5.8 Ma
NU (6.36 ± 0.03 Ma)
6.4 Ma
M (6.88 ± 0.04 Ma)
G (7.03 ± 0.05 Ma)
SL (8.13 ± 0.08 Ma)
0
20
40
60
80
Grass pollen (%)
Tuff ages this paper
Tuff ages from Jones and Lippard (1979)